# Facile Syntheses of a Class of Supramolecular Gelator Following a Combinatorial Library Approach: Dynamic Light Scattering and Small-Angle Neutron Scattering Studies

Parthasarathi Dastidar,*[,†,‡] Satoshi Okabe,[§] Kazunori Nakano,[||] Kouji Iida,[||] Mikiji Miyata,[‡] Norimitsu Tohnai,[‡] and Mitsuhiro Shibayama*[,§]

*Analytical Science Discipline, Central Salt & Marine Chemicals Research Institute, G. B. Marg, Bhavnagar 364 002, Gujarat, India, Material & Life Science, Graduate School of Engineering, Osaka University, Yamodaoka, Suita, Osaka 565-0871, Japan, Neutron Science Laboratory, Institute for Solid State Physics, The University of Tokyo, Tokai, Ibaraki 319-1106, Japan, and Nagoya Municipal Industrial Research Institute, Atsuta-ku, Nagoya, Aichi 456-0058, Japan*

*Received October 13, 2004. Revised Manuscript Received December 3, 2004*

Following a combinatorial library approach, 60 organic salts have been prepared by reacting 5 bile acids and 12 secondary amines. Gelation tests with various organic and aqueous solvents reveal that 16 salts are supramolecular gelators of which 6 salts are found to be ambidextrous displaying the ability to form gels with organic as well as aqueous solvents. The salt didodecylammonium cholate (**1a7b)** is the most versatile gelator, displaying gelation ability with a maximum number of solvents. AFM images of the xerogels of **1a7b** in organic and aqueous solvents reveal the presence of fibrous aggregate including helical fibers. Dynamic and morphological behaviors of the aggregates in the gel state have been probed by dynamic light scattering (DLS) and small-angle neutron scattering (SANS) experiments on an aqueous gel (1:1 DMSO/$H_2O$) of **1a7b**. It is revealed that the gelation takes place via the formation of flexible fibrous clusters followed by physical cross-linking. DLS and SANS results also disclose that (1) the fibrous network is formed via flexible clusters of a few tens of nanometers in length, followed by immobile network formation; (2) the network structure is self-similar irrespective of gelator concentration, *C*, while the gelation temperature is *C* dependent; and (3) the fibrous aggregates are in the solid state with a sharp boundary.

## Introduction

Low molecular mass organic gelators (LMOGs)[1−7] are organic molecules capable of immobilizing organic or aqueous solvents when a solution containing a small amount of LMOG is cooled below its gelation temperature ($T_g$). The resultant viscoelastic solidlike material is termed a gel. Various types of supramolecular aggregates such as fibers, strands, and tapes arising from noncovalent interactions among the gelator molecules are known to cross-link among

* Authors to whom correspondence should be addressed. E-mail: sibayama@iisp.u-tokyo.ac.jp (M.S.); parthod123@rediffmail.com or dastidar@csmcri.org (P.D.).

† Central Salt & Marine Chemicals Research Institute.

‡ Osaka University.

§ The University of Tokyo.

|| Nagoya Municipal Industrial Research Institute.

(1) (a) Terech, P.; Weiss, R. G. *Chem. Rev.* **1997**, *97*, 3133. (b) Prost, J.; Rondelez, F. *Nature* **1991**, *350*, 11 (supplement). (c) van Esch, J.; Feringa, B. L. *Angew. Chem., Int. Ed.* **2000**, *39*, 2263. (d) Abdallah, D. J.; Weiss, R. G. *Adv. Mater.* **2000**, *12*, 1237. (e) Grownwald, O.; Shinkai, S. *Chem. Eur. J.* **2000**, *7*, 4328. (f) Tiller, J. C. *Angew. Chem., Int. Ed.* **2003**, *42*, 3072. (g) Menger, F. M.; Peresypkin, A. V. *J. Am. Chem. Soc.***2003**, *125*, 5340. (h) Menger, F. M.; Yamasaki, Y.; Catlin, K. K.; Nishimi, T. *Angew. Chem., Int. Ed. Engl.* **1995**, *34*, 585. (i) Kölbel, M.; Menger, F. M. *Chem. Commun.* **2001**, 275. (j) Heeres, A.; van der Pol, C.; Stuart, M.; Friggeri, A.; Feringa, B. L.; van Esch, J. *J. Am. Chem. Soc.* **2003**, *125*, 14252. (k) Abdallah, D. J.; Weiss, R. G. *Chem. Mater.* **2000**, *12*, 406. (l) Wang, C.; Robertson, A.; Weiss, R. G. *Langmuir* **2003**, *19*, 1036. (m) Gronwald, O.; Shinkai, S. *Chem. Eur. J.* **2001**, *7*, 4329. (n) Wang, R.; Geiger, C.; Chen, L.; Swanson, B.; Whitten, D. G. *J. Am. Chem. Soc.* **2000**, *122*, 2399. (o) Estroff, L. A.; Hamilton, A. D. *Chem. Rev.* **2004**, *104*, 1201. (p) Krishna Kumar, D.; Jose, D. A.; Dastidar, P.; Das, A. *Langmuir* **2004**, *20*, 10413.

(2) Steroid-based gelators: (a) Lin, Y.; Kachar, B.; Weiss, R. G. *J. Am. Chem. Soc.* **1989**, *111*, 5542. (b) Maitra, U.; Mukhopadhyay, S.; Sarkar, A.; Rao, P.; Indi, S. S. *Angew. Chem, Int. Ed.* **2001**, *40*, 2281. (c) Kawano, S.; Fujita, N.; van Bommel, K. J. C.; Shinkai, S. *Chem. Lett.* **2003**, *32*, 12. (d) Numata, M.; Shinkai, S. *Chem. Lett.* **2003**, *32*, 308.

(3) Carbohydrate-based gelators: (a) Inoue, K.; Ono, Y.; Kanekiyo, Y.; Kiyonaka, S.; Hamachi, I.; Shinkai, S. *Chem. Lett.* **1999**, 225. (b) Bhattacharya, S.; Ghanashyam Acharya, S. N. *Chem. Mater.* **1999**, *11*, 3504. (c) Yamasaki, S.; Tsutsumi, H. *Bull. Chem. Soc. Jpn.* **1996**, *69*, 561. (d) Friggeri, A.; Gronwald, O.; van Bommel, K. J. C.; Shinkai, S.; Reinhoudt, D. N. *J. Am. Chem. Soc.* **2002**, *124*, 10754. (e) Hafkamp, R. J. H.; Kokke, B. P. A.; Danke, I. M.; Geurts, H. P. M.; Rowan, A. E.; Feitersa, M. C.; Nolte, R. J. M.*Chem. Commun.* **1997**, 545.

(4) Anthryl-based gelator: (a) Brotin, T.; Utermohlen, R.; Fages, F.; Bouas-Laurent, H.; Desvergne, J.-P. *J. Chem. Soc., Chem. Commun.* **1991**, 416. (b) Lescanne, M.; Collin, A.; Mondain-Monval, O.; Fages, F.; Pozzo, J.-L. *Langmuir* **2003**, *19*, 2013−2020.

(5) Urea-based gelator: (a) Schoonbeek, F. S.; van Esch, J.; Hulst, R.; Kellog, R. M.; Feringa, B. L. *Chem. Eur. J.* **2000**, *6*, 2633. (b) Shi, C.; Huang, Z.; Kilic, S.; Xu, J.; Enick, R. M.; Beckmann, E. J.; Carr, A. J.; Melendez, R. E.; Hamilton, A. D. *Science* **1999**, *286*, 1540. (c) van Gorp, J. J.; Vekemans, Jef. A. J. M.; Meijer, E. W. *J. Am. Chem. Soc.* **2002**, *124*, 14759. (d) Yabuuchi, K.; Marfo-Owusu, E.; Kato, T. *Org. Biomol. Chem.* **2003**, *1*, 3464. (e) de Loos, M.; van Esch, J.; Kellogg, R. M.; Feringa, B. L. *Angew. Chem., Int. Ed.* **2001**, *40*, 613.

(6) Two-component gelator: (a) Maitra, U.; Vijay Kumar, P.; Chandra, N.; D'Souza, L. J.; Prasanna, M. D.; Raju, A. R. *Chem. Commun.* **1999**, 595. (b) Partridge, K. S.; Smith, D. K.; Kykes, G. M.; McGrail, P. T. *Chem. Commun.* **2001**, 319. (c) Babu, P.; Sangeetha, N. M.; Vijaykumar, P.; U. Maitra, Rissanen, K.; Raju, A. R. *Chem. Eur. J.* **2003**, *9*, 1922. (d) Kawano, S.; Fujita, N.; Shinkai, S. *Chem. Commun.* **2003**, 1352.

10.1021/cm048210o CCC: $30.25 
Published on Web 01/28/2005

themselves through junction zones[8] to form a three-dimensional network within which the solvents molecules are immobilized resulting in gel formation. Unlike polymeric gels whose 3D network is based on covalent linkage, these physical gels obtained from LMOGs depend on relatively weak nonbonded interactions, e.g., hydrogen bonding, $\pi-\pi$ stacking, and van der Waals. Two distinct categories of gelators based on LMOGs, hydrogen bond based and non hydrogen bond based gelators, are known according to the difference in driving force for the molecular aggregation. Research on LMOG has been intensified in recent years due to the challenge involved in the design and synthesis of a gelator molecule as well as its various potential applications in materials science.[9] However, designing a gelator molecule is still a daunting task, and it is also impossible to select a molecule that will definitely gel a selected liquid. Moreover, making most of such gelators involves nontrivial organic synthesis.

Organic salts are increasingly found to be popular in LMOG research[10] since the preparation of such salts does not involve time-consuming nontrivial organic syntheses and in a relatively short period of time many salts can be prepared and scanned for their gelation ability. Moreover, the supramolecular self-assembly in such salts is based on strong and directional hydrogen bonding as well as stronger but less directional electrostatic interactions between the cations and anions.

Structural studies indicate that a 1D hydrogen-bonded network promotes gelation whereas 2D and 3D networks either produce a weak gel or do not promote gelation at all.[11] We have also recently demonstrated that a 1D network is indeed important for the gelation ability of a new class of gelators based on secondary ammonium cinnamate salts.[10b] If one considers the plausible hydrogen-bonding motif of secondary ammonium salts of a monocarboxylic acid, two main motifs, one 1D polymeric and the other cyclic (0D) network through N−H···O hydrogen bonding, can be envisaged[12] (Chart 1).

**Chart 1**

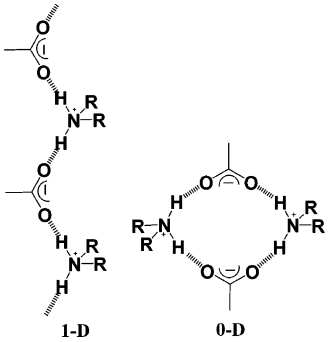


Bile acids are naturally occurring steroidal monocarboxylic acids having unique bent geometry with hydrophobic and hydrophilic molecular surface (Scheme 1) and displaying

**Scheme 1**

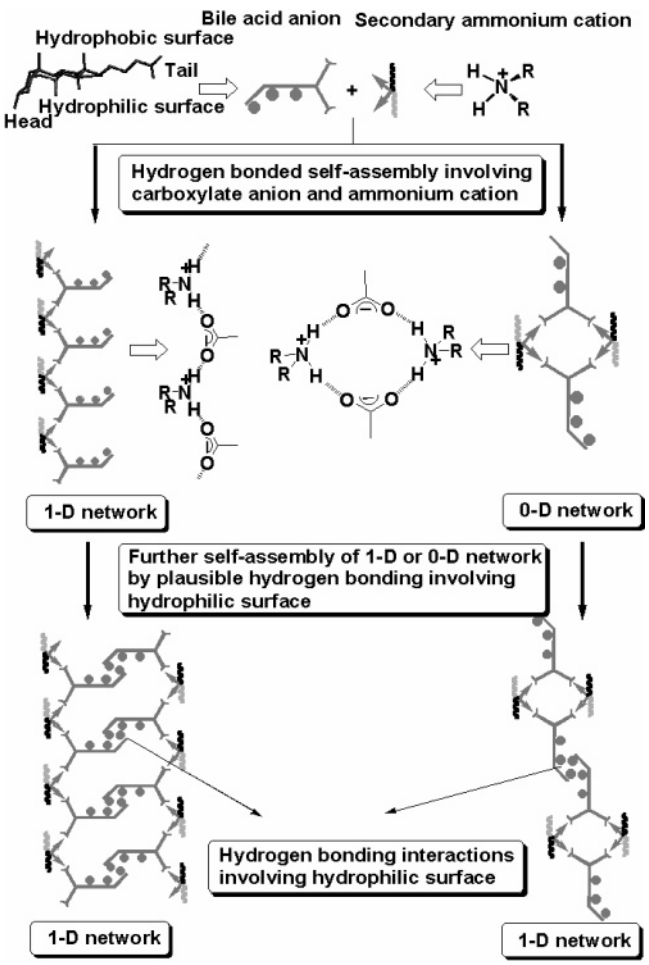


(7) Amino acid/peptide-based gelator: (a) de Vires, E. J.; Kellogg, R. M. *J. Chem. Soc., Chem. Commun.* **1993**, 238. (b) Bhattacharya, S.; Ghanashyam Acharya, S. N.; Raju, A. R. *Chem. Commun.* **1996**, 2101. (c) Hanabusa, K.; Okui, K.; Karaki, K.; Koyama, T.; Shirai, H. *J. Chem. Soc. Chem., Commun.* **1992**, 1371. (d) Hanabusa, K.; Naka, Y.; Koyama, T.; Shirai, H. *J. Chem. Soc., Chem. Commun.* **1994**, 2683. (e) Makerević, J.; Jokić, M.; Frkaneć, L.; Kalalenić, D.; Žinić, M. *Chem. Commun.* **2002**, 2238. (f) Ihara, H.; Takafuji, M.; Sakurai, T.; Katsumoto, M.; Ushijima, N.; Shirosaki, T.; Hachisako, H. *Org. Biomol. Chem.* **2003**, *1*, 3004. (g) Schneider, J. P.; Pochan, D. J.; Ozbas, B.; Rajagopal, K.; Pakstis, L.; Kretsinger, J. *J. Am. Chem. Soc.* **2002**, *124*, 15030. (h) Suzuki, M.; Nakagima, Y.; Yumoto, M.; Kimura, M.; Shirai, H.; Hanabusa, K. *Langmuir* **2003**, *19*, 8622−8624.

(8) (a) Terech, P.; Ostuni, E.; Weiss, R. G. *J. Phys. Chem.* **1996**, *100*, 3759. (b) Terech, P.; Furman, I.; Weiss, R. G. *J. Phys. Chem.* **1996**, *99*, 9958 and references therein.

(9) (a) Bhattacharya, S.; Krishnan-Ghosh, Y. *Chem. Commun.* **2001**, 185. (b) Kobayashi, S.; Hamasaki, N.; Suzuki, M.; Kimura, M.; Shirai, H.; Hanabusa, K. *J. Am. Chem. Soc.* **2002**, *124*, 6550. (c) Jung, J. H.; Ono, Y.; Hanabusa, K.; Shinkai, S. *J. Am. Chem. Soc.* **2000**, *122*, 5008. (d) Trivedi, D. R.; Ballabh, A.; Dastidar, P. *Chem. Mater.* **2003**, *15*, 3971. (e) Sugiyasu, K.; Fujita, N.; Shinkai, S. *Angew. Chem., Int. Ed.* **2004**, *43*, 1229. (f) Yoshimura, I.; Miyahara, Y.; Kasagi, N.; Yamane, H.; Ojida, A.; Hamachi, I. *J. Am. Chem. Soc.* **2004**, *126*, 12204. (g) Kiyonaka, S.; Sada, K.; Yoshimura, I.; Shinkai, K. N.; Hamachi, I. *Nat. Mater.* **2004**, *3*, 58. (h) Numata, M.; Asai, M.; Kaneko, K.; Hasegawa, T.; Fujita, N.; Kitada, Y.; Sakurai, K.; Shinkai, S. *Chem. Lett.* **2004**, *33*, 232.

(10) (a) Ballabh, A.; Trivedi, D. R.; Dastidar, P. *Chem. Mater.* **2003**, *15*, 2136. (b) Trivedi, D. R.; Ballabh, A.; Dastidar, P.; Ganguly, B. *Chem. Eur. J.* **2004**, *10*, 5311. (c) Nakano, K.; Hishikawa, Y.; Sada, K.; Miyata, M.; Hanabusa, K. *Chem. Lett.* **2000**, 1170. (d) Ayabe, M.; Kishida, T.; Fujita, N.; Sada, K.; Shinkai, S. *Org. Biomol. Chem.* **2003**, *1*, 2744. (e) Oda, R.; Huc, I.; Candau, S. J. *Angew. Chem., Int. Ed. Engl.* **1998**, *37*, 2689. (f) Abdallah, D. J.; Weiss, R. G. *Chem. Mater.* **2000**, *12*, 406. (g) George, M.; Weiss, R. G. *J. Am. Chem. Soc.* **2001**, *11*, 10393. (h) George, M.; Weiss, R. G. *Langmuir* **2003**, *19*, 1017.

(11) (a) Luboradzki, R.; Gronwald, O.; Ikeda, M.; Shinkai, S.; Reinhoudt, D. N. *Tetrahedron* **2000**, *56*, 9595. (b) Tamaru, S.-I.; Luboradzki, R.; Shinkai, S. *Chem. Lett.* **2001**, 336.

(12) Biradha, K.; Dennis, D.; MacKinon, V. A.; Sharma, C. V. K.; Zaworotko, M. J. *J. Am. Chem. Soc.* **1998**, *120*, 11894.

interesting lattice inclusion behavior.[13] The hydrogen-bonding sites are located in the hydrophilic surface and the carboxylic end (tail) of the bile acid molecule.

We have decided to investigate secondary ammonium salts of bile acids as potential gelators for the following reasons: (i) many gelators are known to contain a steroidal moiety,[2] (ii) the plausible hierarchical supramolecular self-assembly of the ion pair in such salts may be envisaged as a 1D network irrespective of their primary supramolecular aggregates (either 0D or 1D motif) as depicted in Scheme 1, and (iii) the alkyl chains (specially long chain) in the cation are expected to help aggregate further the 1D network of ion pairs through hydrophobic (alkyl−alkyl) interactions.

Dynamic light scattering (DLS) is a nondestructive method to study the gelation process.[14] For this reason, DLS has been successfully used to study the gelation process for various systems including acrylamide and its derivatives,[15] gelatin,[16] siloxanes,[17] and $\beta$-globulin.[18] The common features of gelation are an abrupt increase in the scattering intensity and appearance of nonergodicity. The time−intensity correlation function exhibits a characteristic broadening of the relaxation time with a power law fashion.[14] Small-angle neutron scattering (SANS) is also extensively utilized to investigate the structure of gels.[19] In particular, physical gels made with organic gelators often show a fibrous structure with a large aspect ratio.[20,21] Therefore, it is of particular importance to combine both the methods to elucidate the structure and gelation mechanism of gels derived from organic gelators.

In this report, we present the preparation, gelation characteristics, optical microscopy, AFM, DLS, and SANS studies of a new class of LMOG based on secondary ammonium salts of bile acids obtained by combinatorial library approach.

## Experimental Section

**Materials and Physical Measurements.** All chemicals are commercially available (Aldrich and TCI) and used without further purification. FT-IR spectra are recorded using a Horiba FT-720 spectrometer. A Hirox digital optical microscope fitted with crossed polars is used to observe the aggregates in the gel state. Fibers in the xerogel are observed using JSPM-4210 (JEOL) AFM instruments.

**Preparation of Salts.** All salts are prepared by mixing equimolar amounts of the corresponding acid and amine in THF followed by the evaporation of the solvent in a rotary evaporator. The resultant white solid is isolated as the salt in a near-quantitative yield. FT-IR spectra (KBr) of the salts show the presence of an asymmetric stretching band of the carboxylate group ($COO^-$) at ~1558 $cm^{-1}$ and the absence of a carbonyl stretching band (C═O) of COOH at ~1704−1735 $cm^{-1}$ indicating complete salt formation.

**Optical Microscopy.** A drop of 10 $\mu$L of solution containing the gelator molecule is placed on a glass plate and allowed to form a gel, which is then observed under a Hirox optical microscope equipped with crossed polars. The photographs of the gel fibers are acquired digitally.

**Atomic Force Microscopy.** The gels are prepared from the salts in water with a few drops of methanol (10 wt %), in 1:1 (v/v) water/DMSO solution (1 wt %) and in nitrobenzene (5 wt %). Then the gels are dried on a glass plate at low pressure. Imaging is performed with a commercial JSPM-4210 (JEOL) equipped with a standard silicon probe (BS-Multi 75Al, 3 N/m) using an ac mode (tapping mode).

**Dynamic Light Scattering.** DLS experiments are carried out on ALV/DLS/SLS-5000-F compact goniometer system (Langen, Germany). A He−Ne laser with the wavelength of 632.8 nm is used as an incident beam. The scattered photons are collected with an avalanche photodiode system, and the scattered intensity is obtained as the counting rate of the photons. An intensity−time correlation function (ICF) is calculated as a convolution of the scattered intensity. The typical measuring time is 30 s. The scattering angle is 90°. For the sake of determining the gelation points, the scattered light intensity is monitored as a function of temperature. The temperature of the sample is carefully controlled with a water circulating system (RTE-111M, Neslab, Co., Ltd., Newton, MA). The temperature is fixed during measurements with the precision of 0.1 °C and then lowered to below the gelation points step by step.

**Small-Angle Neutron Scattering.** SANS experiments are carried out at the SANS-U spectrometer (The University of Tokyo, Tokai, Japan). The wavelength of the incident neutron beam is 0.7 nm. Scattered neutrons are collected with an area detector of 64 cm × 64 cm (Ordela, 2660N). The samples are loaded in quartz cells with the thickness of 1 mm for 1 and 5 wt % samples and 2 mm for 0.1 and 0.5 wt % samples. Standard data reduction such as subtraction of the cell scattering and division by the sample thickness is carried out. The scattered intensity is scaled to the absolute intensity with the incoherent scattering from a polyethylene secondary standard sample, and then subtraction of the incoherent scattering from the solute and the solvent is performed. The temperature of the samples is controlled with a Neslab, RTE−111 and a programmable heating system with a stability of 0.01 °C.

## Theoretical Background

**DLS.** The dynamics of polymer solutions can be investigated by taking ICF as a function of decay time, $\tau$. The ICF, $g^{(2)}(\tau)$, is given by

$$g^{(2)}(\tau) \equiv g^{(2)}(\tau;q) = \frac{\langle I(0;q)I(\tau;q)\rangle_T}{\langle I(0;q)\rangle_T^2} = |g^{(1)}(\tau;q)|^2 + 1 \quad (1)$$

where $\langle I(\tau;\ q)\rangle_T$ is the scattering intensity at time $\tau$ with respect to $\tau = 0$ and the scattering vector $q$, and $\langle\cdots\rangle_T$ denotes a time average. $g^{(1)}(\tau)$ is the scattering field time correlation function given by a Laplace transform of the characteristic decay time distribution function, $G(\Gamma)$, i.e.,

$$g^{(1)}(\tau) = \int_0^\infty G(\Gamma)\exp(-\Gamma\tau)\,d\Gamma \quad (2)$$

(13) (a) Miyata, M.; Sada, K. In *Comprehensive Supramolecular Chemistry*; MacNicol, D. D., Toda, F., Bishop, R., Eds.; Pergamon Press: Oxford, 1996; Vol. 6, Chapter 6, p 147. (b) Dastidar, P. *CrystEngComm* **2000**, 8. (c) Miyata, M.; Sada, K.; Yoswathananont, N. In *Encyclopedia of Supramolecular Chemistry*; Atwood, J. L., Steed, J. W., Eds.; M. Dekker: New York, 2004; Vol. 1, p 441. (d) Sada, K.; Shiomi, N.; Miyata, M. *J. Am. Chem. Soc.* **1998**, *120*, 10543.
(14) Shibayama, M.; Norisuye, T. *Bull. Chem. Soc. Jpn.* **2002**, *75*, 641.
(15) Norisuye, T.; Shibayama, M.; Nomura, S. *Polymer* **1998**, *39*, 2769.
(16) Okamoto, M.; Norisuye, T.; Shibayama, M. *Macromolecules* **2001**, *34*, 8496.
(17) Norisuye, T.; Inoue, M.; Shibayama, M.; Tamaki, R.; Chujo, Y. *Macromolecules* **2000**, *33*, 900.
(18) Takata, S.; Norisuye, T.; Tanaka, N.; Shibayama, M. *Macromolecules* **2000**, *33*, 5470.
(19) Shibayama, M. *Macromol. Chem. Phys.* **1998**, *199*, 1.
(20) Terech, P.; Coutin, A.; Giroud-Godquin, A. M. *J. Phys. Chem. B* **1997**, *101*, 6810.
(21) Terech, P.; Allegraud, J. J.; Garner, C. M. *Langmuir* **1998**, *14*, 3991.

where $\Gamma^{-1}$ is the characteristic decay time. In the case of gels, the scattering intensity strongly fluctuates with sample position. Each speckle corresponds to time-average scattering intensity, $\langle I \rangle_T$. On the other hand, an ensemble-average scattering intensity, $\langle I \rangle_E$, is obtained by taking an average over the sample positions. The inequality, i.e.,

$$\langle I \rangle_E \neq \langle I \rangle_T \tag{3}$$

is one of characteristic features of gels. A system in which the ergodic hypothesis does not hold is called a *nonergodic* system. It is known that glasses and gels are nonergodic systems.[23,24] In this case, the ICF obtained at a given position becomes position dependent and the initial amplitude of ICF

$$\sigma_I^2 \equiv \frac{\langle I(0;q)^2 \rangle_T}{\langle I(0;q) \rangle_T^2} - 1 = g_T^{(2)}(0;q) - 1 \tag{4}$$

becomes much less than unity due to the appearance of nonergodicity.

**SANS.** The scattering intensity function, $I(q)$, for randomly oriented rods, diameter $2R$ and length $2H$, is given by[25]

$$I(q) = \int_{\alpha=0}^{\pi/2} \frac{\sin^2(qH\cos\alpha)}{(qH\cos\alpha)^2} \frac{4[J_1(qR\sin\alpha)]^2}{(qR\sin\alpha)^2} \sin\alpha \, d\alpha \tag{5}$$

where $J_1(x)$ is the Bessel function of order 1 and $\alpha$ is the angle between the preferential axis of the rod and the scattering vector. If the length of the rod is much larger than the radius and the rods are randomly oriented in the space, an asymptotic form is obtained as,

$$I(q) \sim 4q^{-2} \frac{[J_1(qR)]^2}{(qR)^2} \sim q^{-3} \tag{6}$$

Hence, $I(q)$ is asymptotically decreasing as a function of $q$ with the power of $-4$ for $q$ greater than $1/R$, where $R$ is the radius of the rod. Equation 6 also indicates that a scattering maximum appears around $R \approx 5.1/q_m$, providing the rods have a sharp distribution in their thickness.

## Results and Discussion

**Preparation of Salts and Their Gelation Behavior.** Sixty salts (Table 1) have been prepared by mixing 5 bile acids (Chart 2a) and 12 secondary amines (Chart 2b) following a combinatorial library approach. Except in ursodeoxycholic acid (**5a**), the hydroxyl groups in the bile acids chosen for this study are sterically arranged in the same direction making the somewhat concave surface of the molecule hydrophilic and potential hydrogen-bonding site. In the case of **5a**, the hydroxyl groups are oriented in the opposite direction making both the surfaces of the molecule rather similar in nature. It may be noted here that among the acids chosen for this study, cholic acid (**1a**) has highest number of hydroxyl groups making its hydrophilic surface more susceptible toward hydrogen bonding. The alkyl chains of the amines **1b**−**7b** are systematically varied to see its effect on gelation. The effect of other substituents on gelation has also been investigated by choosing amines, namely, **3b′**, **5b′**, **8b**, **9b**, and **10b**, containing various types of substituents (Chart 2b). The italic cells of Table 1 depict the salts capable of gelling 1 or more solvents out of the 12 solvents tested in this study. It is clear from Table 1 that out of 60 salts prepared, 16 of them show gelation ability. Table 2 shows the details of the gelation behavior of these 16 salts. The gelators appear to be capable of gelling only polar solvents. Salt **1a7b**, which is capable of gelling the maximum number of solvents,

**Table 1. Combinatorial Library of the Secondary Ammonium Bile Acid Salts[a]**

| | 1a | 2a | 3a | 4a | 5a |
|---|---|---|---|---|---|
| **1b** | 1a1b | 2a1b | 3a1b | *4a1b* | 5a1b |
| **2b** | 1a2b | 2a2b | 3a2b | 4a2b | 5a2b |
| **3b** | *1a3b* | 2a3b | 3a3b | 4a3b | 5a3b |
| **3b′** | 1a3b′ | 2a3b′ | 3a3b′ | 4a3b′ | 5a3b′ |
| **4b** | 1a4b | 2a4b | 3a4b | 4a4b | 5a4b |
| **5b** | 1a5b | *2a5b* | 3a5b | 4a5b | 5a5b |
| **5b′** | 1a5b′ | 2a5b′ | 3a5b′ | *4a5b′* | 5a5b′ |
| **6b** | *1a6b* | *2a6b* | 3a6b | 4a6b | *5a6b* |
| **7b** | *1a7b* | *2a7b* | *3a7b* | *4a7b* | *5a7b* |
| **8b** | *1a8b* | 2a8b | 3a8b | 4a8b | 5a8b |
| **9b** | 1a9b | 2a9b | 3a9b | 4a9b | 5a9b |
| **10b** | 1a10b | 2a10b | 3a10b | *4a10b* | 5a10b |

[a] The salts in italic type are gelators.

**Chart 2**

**Preparation of salts and their gelation behavior:**

**(a)**

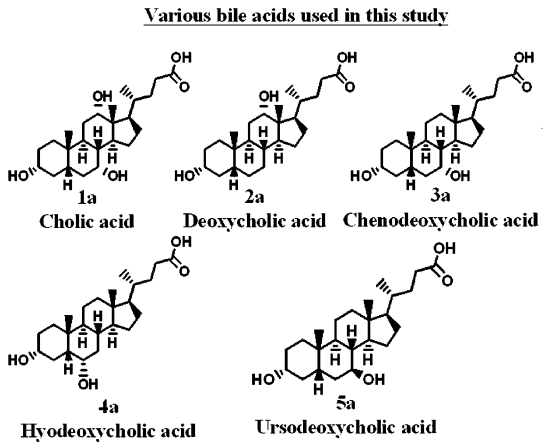


**(b)**

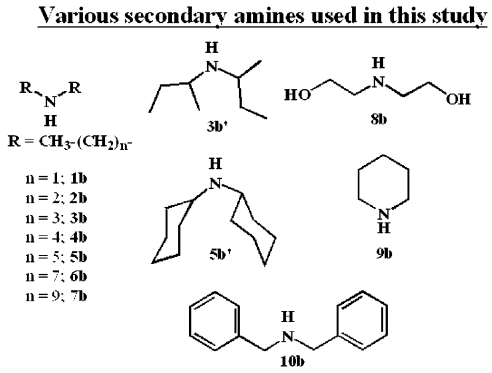


(22) Tanaka, T.; Hocker, L. O.; Benedek, G. B. *J. Chem. Phys.* **1973**, *59*, 5151.
(23) Pusey, P. N.; van Megen, W. *Physica A* **1989**, *157*, 705.
(24) Xue, J. Z.; Pine, D. J.; Milner, S. T.; Wu, X. L.; Chaikin, P. M. *Phys. Rev. A* **1992**, *46*, 6550.
(25) Fournet, G. *Bull. Soc. Franc. Mineral. Crist.* **1951**, *74*, 39.

**Table 2. Gelation Data**[a]

| solvents | 1a3b | 1a5b | 1a6b | 1a7b | 1a8b | 2a5b | 2a6b | 2a7b | 3a7b | 4a1b | 4a4b | 4a5b′ | 4a7b | 4a10b | 5a6b | 5a7b |
|---|---|---|---|---|---|---|---|---|---|---|---|---|---|---|---|---|
| nitrobenzene | P | P | *VL* | *G/1* | *VL* | S | S | S | S | P | P | P | P | G/10 | P | P |
| toluene | S | S | P | *VL* | *VL* | S | S | S | P | P | P | P | P | S | P | P |
| *p*-xylene | S | S | S | S | S | S | S | S | S | P | P | P | P | S | P | P |
| *m*-xylene | S | S | S | P | S | S | S | S | S | P | P | P | P | P | P | P |
| mesitylene | S | S | S | S | P | S | S | S | S | P | P | P | P | P | P | P |
| DMSO | *G/10* | *G/5* | *G/2.5* | *G/1* | S | *G/10* | *G/10* | *G/10* | *G/10* | S | *G/2.5* | P | *G/10* | S | *G/10* | *G/10* |
| DMF | S | S | *G/10* | *G/2.5* | S | S | S | *G/10* | *G/10* | S | S | S | S | S | P | P |
| acetophenone | S | S | S | *G/1* | S | P | P | S | S | S | S | *LG* | S | *G/10* | S | P |
| anisole | S | S | S | *G/0.5* | S | P | S | S | S | P | S | P | S | *G/5* | P | P |
| *n*-decane | S | S | S | S | S | S | S | S | S | S | S | S | S | S | S | P |
| chlorobenzene | S | S | S | *VL* | S | S | S | S | S | P | P | P | S | *G/2.5* | S | P |
| methylbenzoate | S | S | S | *G/2* | *G/2.5* | P | S | S | S | *G/0.5* | P | *G/5* | S | *G/2.5* | S | P |
| DMSO/$H_2O$ (1:1) | S | P | *G/2* | *G/0.5* | *G/2* | *LG* | S | S | S | S | S | *G/2* | S | P | *G/2* | *G/2* |

[a] G = gel; S = solution; P = precipitate; VL = viscous liquid; LG = loose gel. The numerical values indicate the minimum gelator concentration in wt % (w/v); the italic type is used to highlight gels, VL or LG.

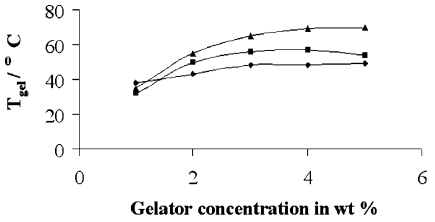


**Figure 1.** $T_{gel}$ vs gelator concentration plot of **1a7b** gel in (▲) DMSO/water (1:1, v/v), (■) in nitrobenze, or (◆) in anisole. $T_{gel}$ is determined by the drop-ball method.[10b]

appears to be the best among the lot prepared. It is also apparent that both long alkyl chains and maximum number of hydroxyl groups oriented in the same direction, as in the case of **1a7b**, are important for efficient gelation. It is notable that six salts, **1a6b**, **1a7b**, **1a8b**, **4a5b′**, **5a6b,** and **5a7b**, are ambidextrous displaying a rare ability to gel both organic and aqueous solvents. Salt **1a7b** is also capable of gelling pure water at high concentration (10 wt %). Since **1a7b** is the most efficient gelator and gels at low concentration are transparent, further studies are carried out with this gelator.

To compare the thermal stability of the gel of **1a7b** in anisole, nitrobenzene. and DMSO/water (1:1, v/v), a plot of gel−sol dissociation temperature ($T_{gel}$) against gelator concentration is examined (Figure 1). The increase of $T_{gel}$ with the increase of gelator concentration indicates that the self-assembly in the gel state is driven by strong intermolecular interactions. It is also noted that gel in aqueous solvent is the strongest one among the three solvents compared.

**Microscopy.** To see the feature of the aggregates in the gel state, optical microscopy is performed on a gel of **1a7b** (5 wt %, in DMSO/water (1:1, v/v)). Intertwined network of several micrometer-long fibers, often branched, are easily seen in the optical micrograph (Figure 2).

To see further details of the fibers at high resolution, AFM images are recorded on xerogels of **1a7b** (Figure 3). Fibrous network with submicrometer-size fibers (diameter ∼0.055 $\mu$m or smaller) can be seen in the xerogel obtained from 5 wt % gel in DMSO/water (1:1, v/v). The small fibers apparently weave into larger bundles of fiber (diameter, ∼0.165 $\mu$m) that have a distinct helical pitch (Figure 3a). Fibers with wide range of dimension (diameter, ∼0.22−1.5 $\mu$m) are present in the xerogel prepared from 10 wt % gel

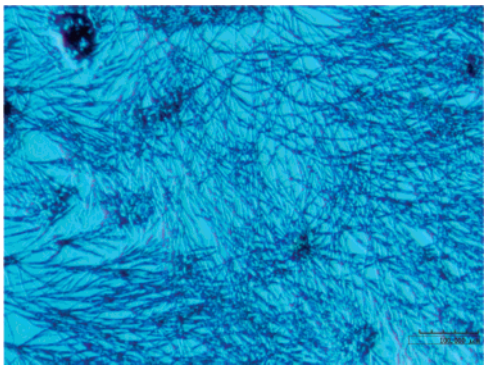

**Figure 2.** Optical micrograph of the intertwined network of fibers in the gel of **1a7b** (5 wt % in 1:1 DMSO/water, v/v) (bar 100 $\mu$m).

in water (Figure 3b). Whereas the nitrobenzene xerogel prepared from 5 wt % gel shows intertwined network of fibers with diameter of ∼0.12 $\mu$m often bundled to form thicker fibers (Figure 3c). It is interesting to note that, only in the case of DMSO/water gel, twisted or helical fiber can be seen.

It may be noted here that X-ray powder diffraction experiments indicate that both bulk solid and xerogels of **1a7b** are amorphous in nature. This could be due to the loss of entrapped solvent molecules from the crystalline lattice during bulk solid or xerogel formation. Since bile acid and its salts are known to form inclusion complex,[13] this observation is not unlikely. Since both DLS and SANS are nondestructive methods and most suitable to study gel formation in its native state, further studies are carried out to see the insights into the dynamic and morphological behavior of the aggregate in the gel state.

**DLS.** Figure 4 shows the variation of the time-averaged scattered intensity, $\langle I \rangle_T$, during cooling process. The gelator concentration, $C$, is 0.5 wt %, and the cooling rate is fixed at 0.1 °C/min. As clearly shown, $\langle I \rangle_T$ increases drastically at ∼2.3 h from the start of cooling and, after a while, $\langle I \rangle_T$ starts to fluctuate. As discussed in Theoretical Background, the abrupt increase and the fluctuations of $\langle I \rangle_T$ are generally observed in gelation processes in many kinds of systems.[14] It may be noted here that the decrease in $\langle I \rangle_T$ for $t > 3.5$ h is due to the opaqueness of the sample.

Figure 5a shows the variation of the initial amplitude of the intensity correlation function, $\sigma_I^2$, during the cooling

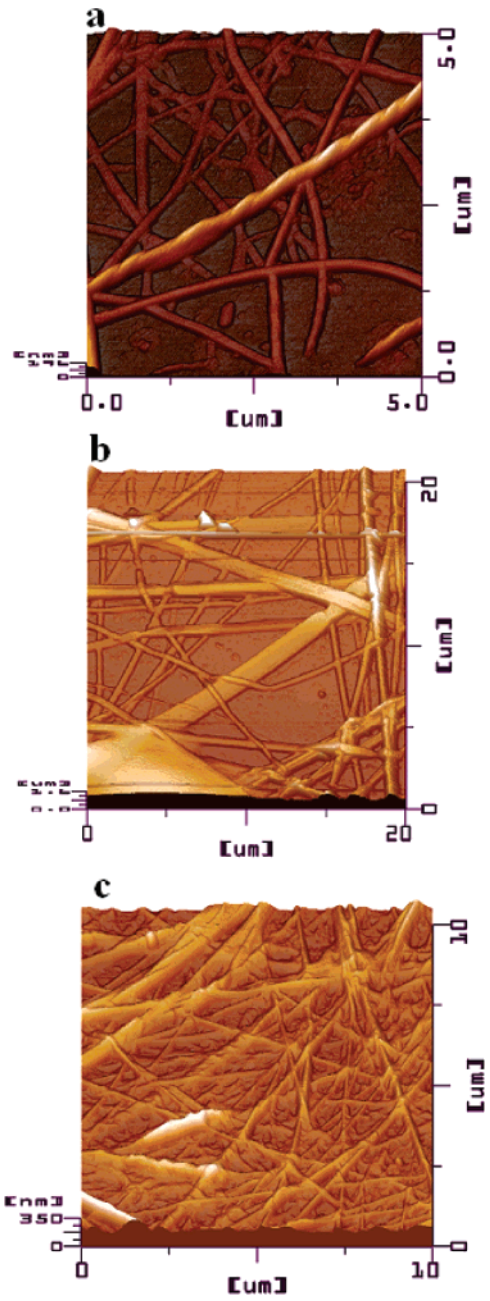


**Figure 3.** AFM micrographs of the xerogels of **1a7b**: (a) 5 wt % in DMSO/water (1:1, v/v), (b) 10 wt % in water, and (c) 5 wt % in nitrobenzene.

process ($C$ = 0.5 wt %; cooling rate, 0.1 °C/min.). It is clearly indicated that the gelation process can be classified to three stages, i.e., (i) induction stage (stage I; $T > T_a$), (ii) association stage (stage II; $T_a > T > T_{g,DLS}$), and (iii) freezing stage of the network (stage III; $T_{g,DLS} > T$), where $T_a$ is the temperature of starting association and $T_{g,DLS}$ the gelation temperature determined by DLS. Some typical examples of the intensity correlation function, $g^{(2)}(\tau)$, and the distribution function of the decay rate, $G(\Gamma)$, are shown in Figure 5b−d.

$G(\Gamma)$'s at each point are obtained with a so-called CONTIN (constraint regulation method) method.[26] The position of the slope in $g^{(2)}(\tau)$ or the peak in $G(\Gamma)$ indicates the decay time of the relaxation mode. In stage I, $\sigma_I^2$ is

(26) Peters, R. In *Dynamic Light Scattering: The Methods and some Applications*; Brown, W., Ed.; Oxford University Press: Oxford, 1993.

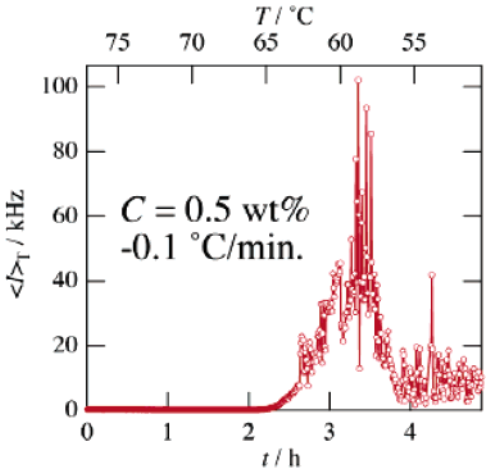


**Figure 4.** Variation of the time-averaged light scattered intensity, $\langle I \rangle_T$.

strongly scattered because the scattered light has no time correlation. This indicates that LMOG remains in a dispersed state. In stage II, $\sigma_I^2$ is close to unity, indicating a presence of associated clusters correlating with each other. To our knowledge, it is the first time the stage II, i.e., the association stage, can be observed. The observed relaxation in the correlogram indicates the translational diffusion of the clusters. In this stage, the structure grows gradually via the formation of flexible fibrous clusters having the characteristic relaxation time of ~10 ms, which corresponds to the size of a few tens of nanometers-long fibers. In stage III, $\sigma_I^2$ becomes much less than unity. Hence, this stage is assigned to a frozen network (or a gel state).[14] In addition, the absence of any peak in $G(\Gamma)$ indicates the gel network is frozen. This DLS result is consistent with the macroscopic brittleness of LMOG gels.

These changes in $g^{(2)}(\tau)$ are in good agreement with those in $\langle I \rangle_T$. Note that the change in the transient region between the stages I and II is continuous and that between II and III is rather discontinuous. The former indicates that the strength of the combination between each gelator molecule is governed by a delicate balance between the dominant forces, i.e., hydrogen bonding and thermal fluctuations, and the latter implies that the motion of the gel network is restricted by the stiffness of its unit structure soon after a percolation. A similar result was obtained for the case of lower concentration, i.e., 0.3 wt %. However, DLS measurements at higher concentrations could not be conducted because of the opaqueness of the resulting gel.

**SANS.** Figure 6 shows the variation of SANS profiles, $I(q)$s, for the cooling process of **1a7b** gel in a mixture of d-DMSO and $D_2O$ (1:1, v/v) at various concentrations. At high temperatures, there are no significant scattering and $I(q)$ is $q$-independent for all of the concentrations studied here. However, as temperature decreases, $I(q)$ suddenly increased at low $q$ regions, i.e., $q \leq 0.03$ Å$^{-1}$. Interestingly, $I(q)$ is scaled as

$$I(q) \sim q^{-4} \quad (q \leq 0.03 \text{ Å}^{-1}) \tag{7}$$

In addition, $I(q)$ does not exhibit any scattering maximum. On the other hand, $I(q)$ is $q$ independent for $q > 0.03$ Å$^{-1}$

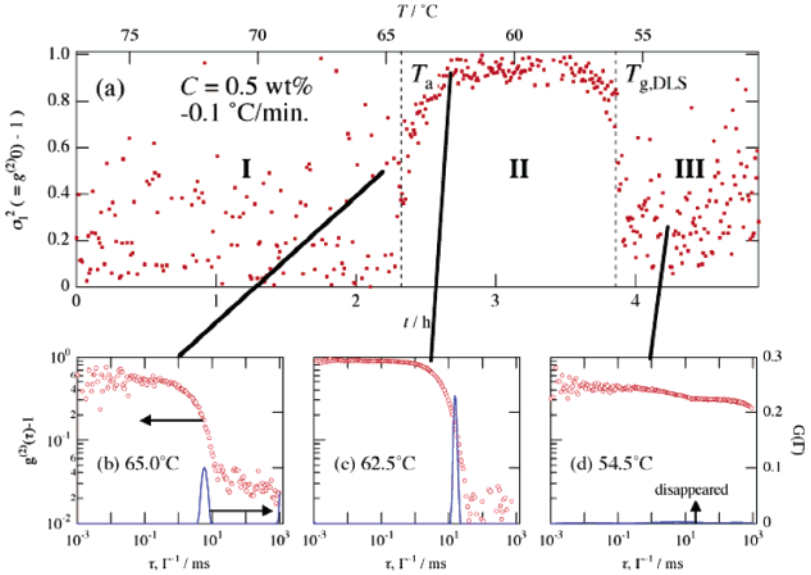


**Figure 5.** (a) Variation of the initial amplitude of the intensity correlation function, $\sigma_I 2$, classified to three stages. The intensity correlation function, $g^{(2)}(\tau)$, and the distribution function of the decay rate, $G(\Gamma)$, (b) at the transient region between stages I and II, (c) in stage II, and (d) stage III.

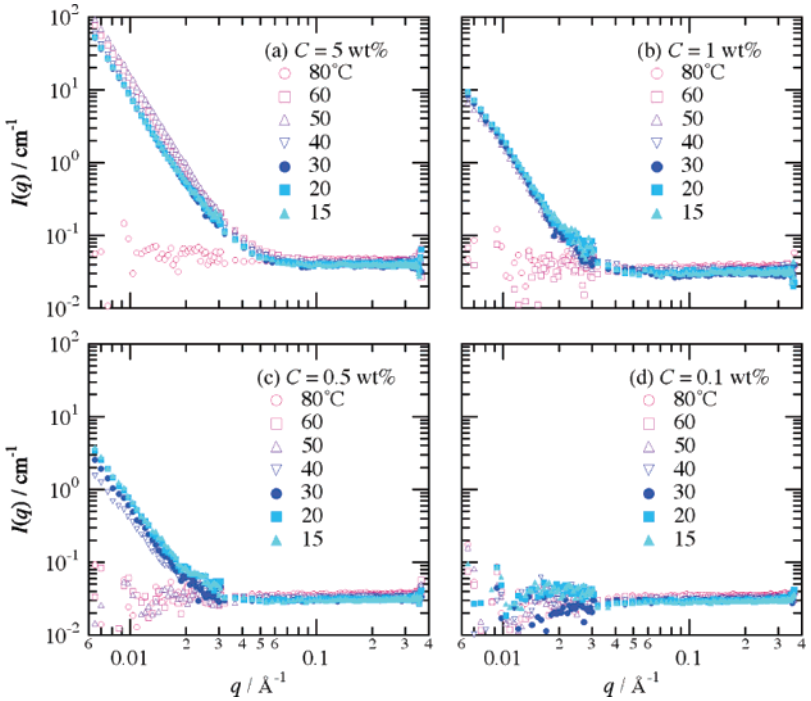


**Figure 6.** Variations of the SANS intensity profiles.

due to incoherent scattering from hydrogen in the system. These observations indicate that the scattering objects consist of a two-phase structure with a sharp boundary (Porod's law)[27,28] and there is no characteristic size in the observation window. By taking account of the AFM observation, we conclude that the scattering objects are rodlike with a broad distribution of the radius.

The temperature at which $I(q)$ abruptly increased is concentration dependent. Figure 7 shows the temperature dependence of the scattering intensity at the lowest $q$, $I(q = 0.0065$ Å$^{-1})$. As shown in the figure, the scattering intensity undergoes an all-or-none transition at a temperature. This temperature corresponds to $T_{g,DLS}$, i.e., the transition from stage II to III. The concentration dependence may suggest that gelation takes place by competition between the cooling rate and the association rate of gelator molecules in the solvent. In other words, the higher the concentration, the higher the association rate resulting in gelation at a higher temperature.

(27) Porod, G. *Kolloid Z.* **1951**, *124*, 83.
(28) Porod, G. *Kolloid Z.* **1952**, *125*, 51.
(29) Terech, P.; Ostuni, E.; Weiss, R. G. *J. Phys. Chem.* **1996**, *100*, 3759.
(30) Okabe, S.; Andoh, K.; Hanabusa, K.; Shibayama, M. *J. Polym. Sci., Part B, Polym. Phys. Ed.* **2004**, *42*, 1841.
(31) Shibayama, M.; Nagao, M.; Okabe, S.; Karino, T. *J. Appl. Crystallogr.*, submitted.

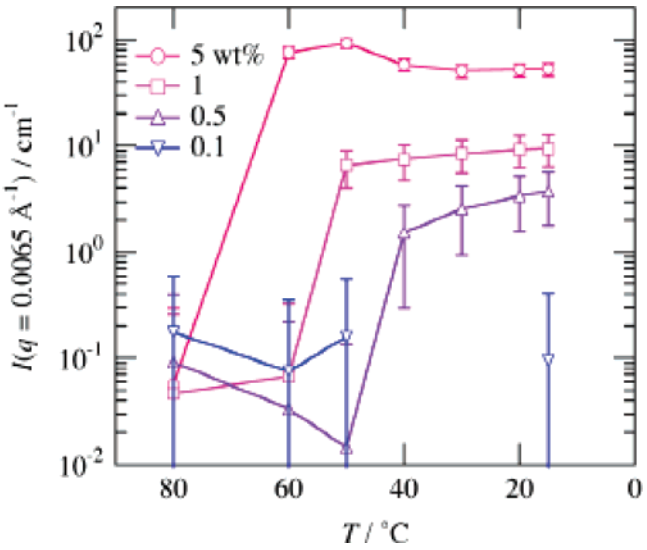


**Figure 7.** Temperature variation of the scattered intensity, $I(q = 0.0065\ \text{Å}^{-1})$.

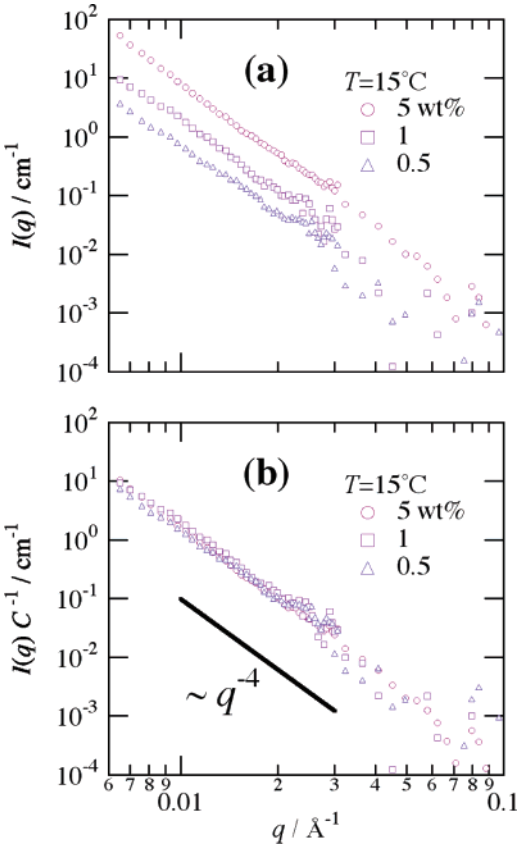


**Figure 8.** (a) $I(q)$'s for $C = 0.5$, 1 and 5 wt % systems after subtraction of incoherent scattering. (b) SANS intensities divided by $C$.

Figure 8a shows $I(q)$s for $C = 0.5$, 1, and 5 wt % LMOG solutions observed at 15 °C. Here, the incoherent scattering arising from hydrogen is subtracted by calculation where multiple scattering form hydrogen containing materials is taken into account.[31] Note that the $q^{-4}$ relationship is clearly observed for all of the concentrations. Figure 8b shows reduced scattering functions with respect to $C$. Interestingly, all the scattering intensity functions are superimposed to each other by scaling with $C$. This indicates that the structures of gels are self-similar irrespective of gelator concentration at least for $C \geq 0.5$ wt %. This also supports the AFM observation, i.e, an assembly of fibrous clusters having a wide range of thickness randomly oriented in the space. Such kinds of assembly of LMOG are also reported in the literature.[20,29,30]

## Conclusions

A combinatorial library of secondary ammonium salts of bile acids has been demonstrated to be a facile preparation method of a new class of gelators. That 1D hydrogen-bonded network promotes gelation whereas the 2D and 3D networks either produce weak gel or do not promote gelation at all seems to be a good working hypothesis. It is also notable that many of the gelators are ambidextrous displaying a rare ability to form gel with both organic and aqueous solvents. From the DLS and SANS investigations, it is concluded that the gelation process can be classified into three stages (I) a dispersion of LMOG molecules (solution), (II) fibrous structures of the associations (pregel), and (III) a pseudoinfinite network (gel). During stage II, the structure grows gradually via formation of flexible fibrous clusters having the characteristic relaxation time of ~10 ms, which corresponds to the size of a few tens of nanometers-long fibers. Soon after percolation, fibrous network with a sharp boundary is formed and the network loses its mobility. SANS results also indicate that the gel network consists of rodlike aggregate with broad distribution of radius, which is in good agreement with the AFM observation.

**Acknowledgment.** Japan Society for the Promotion of Science (JSPS) is thankfully acknowledged for an Invited-JSPS fellowship to P.D. This work was partially supported by the Grant-in-Aid for Scientific Research on Priority Areas (A), "Dynamic Control of Strongly Correlated Soft Materials" (413/14045216) from the Ministry of Education, Science, Sports, Culture, and Technology. The SANS experiment was done under the approval of the Neutron Scattering Program Advisory Committee at Institute for Solid State Physics, The University of Tokyo, Proposal 04-4520.

CM048210O